Estimating Land Surface Temperature from Satellite image: A case study of Mubi Metropolis in Adamawa State Nigeria

Lazarus G. Ndatuwong

Department of Pure and Applied Physics, Adamawa State University, Mubi, P.M.B 25, Adamawa State, Nigeria.
Contact: ndatuwong@gmail.com

Abstract

In the present study, a single thermal infra-red sensor (TIRS) band and two operational land imager (OLI) bands of Landsat 8 were used to estimate the land surface temperature (LST) for Mubi metropolis using the Radiative Transfer Equation (RTE) based method. Applying math algebra in ArcGIS Toolbox to transform the TIRS and OLI bands into spectral radiance and top-of-atmosphere planetary reflectance is the primary task. Using the TIRS band 10, top-of-atmosphere radiance and at-sensor brightness temperature were first calculated. The normalized difference vegetation index (NDVI), the percentage of vegetation (PV), and the land surface emissivity (LSE) are all estimated using OLI bands 4 and 5, which are then converted to the top of the atmosphere's reflectivity. The atmospheric parameters: upwelling and downwelling path radiance with atmospheric transmittance needed for the RTE to estimate the LST were retrieved from an online atmospheric correction calculator available at https://atmcorr.gsfc.nasa.gov/. The study's findings indicate that the average temperature in the studied area varied between 30.85°C and 42.19°C. The estimated LST was classified into two classes, with 51% (or 29.55 square km) of the study area having temperatures that are above average and 49% (or 28.15 square km) of the study region having temperatures that are below average. The outcome of this work was further compared with information on near-surface air temperature received from Adamawa State University's metrological station in Mubi, situated in the study region. The estimated LST was calculated for the pixel where the weather station was located. The LST at the metrological station has a pixel value of roughly 37.55 °C, whereas the metrological data recorded an instantaneous average near-surface air temperature of 30.8 °C on that day.

Keywords: LST, RTE, Landsat 8, Emissivity, Thermal Infra-red and Operational Land Imager

Introduction

The surface temperature of the earth's crust where the heat and radiation from the sun are absorbed, reflected, and refracted is known as Land Surface Temperature (LST). It can be defined as the temperature experienced when the bare hands are placed on the ground or the skin temperature of the ground (Rajeshwari and Mani, 2014). It serves as an important factor for the study of climate change, urban environment, heat balance studies, hydrological and agricultural processes, urban land use and land cover, as well as user input for climate models. It is one of the fundamental variables in the physics of land surface processes on a regional as well as a global scale and a key factor for calculating the highest and lowest temperature of a particular location (Anandababu et. al., 2018). The knowledge of LST is therefore important to a range

of issues and themes in earth sciences, central to urban climatology, global environmental change and human-environment interactions (Javed et. al., 2008). Generally, remote sensing images taken by ground-based, airborne, or satellite-based sensors are typically used to retrieve LST and are very useful in various fields, like astronomy, atmospheric studies, earth observation, communications, navigation, and search and rescue. LST data from airborne and satellite platforms provides a synoptic spatial perspective that can be useful for modelling and tracking environmental processes at various spatial scales (Mutiibwa et. al., 2015).

Remote sensing techniques have emerged as one of the effective tools for systematic survey, analysis, and better management of natural resources (land,

soil, water, forests, mountains) along with the monitoring of desertification, flood, drought, and landform change. It offers a wide range of opportunities to investigate, catalog, and evaluate the natural resources of undeveloped areas. Environmental scientists have become more conscious of the importance of remote sensing in understanding how the connection between man and the environment is evolving as a result of the development of remote sensing and GIS (Sharma and Bisht, 2019; UKEssays, 2018). In terms of surface radiance and emissivity data, remote sensing is helpful for understanding the spatiotemporal land cover change in relation to the basic physical properties (Orhan et. al., 2014).

Many scholars have studied the various methods used for LST retrieval using Landsat thermal infrared images. Among these methods are the mono-window algorithm (MWA), developed by Qin et al., (2001), the split window algorithm (SWA), developed by Becker and Li, (1990), the single-channel algorithm (SCA) method, developed

by Jiménez-Muñoz and Sobrino et al., (2003), and radiative transfer equation method (RTEM) developed by Zhou et.al, (2014). In the present study, the thermal infra-red sensor (TIRS) band 10 and two operational land imager (OLI) bands (4 and 5) were used to estimate the LST for Mubi metropolis using the RTEM method. The RTEM method was employed due to the fact that it was found to be the most accurate model by Yu et al. (2014).

Materials and Methods
Study Area
The study was carried out in Mubi metropolis. According to Adebayo (2004), Mubi metropolis is a geo-political area comprising two Local Government Areas; Mubi North and Mubi South. The metropolis is located between latitudes 10° 12' and 10° 19'N of the equator and between longitude 13° 12' and 13° 19'E of the Greenwich meridian and occupies an area of about 57.699 square km (figure 1).

Figure 1: Study Area; Mubi Metropolis

The dry season and the rainy season are two separate seasons that the study region experiences. While the rainy season begins in May and lasts

until October, the dry season lasts from November to April. The amount of precipitation per year ranges between 700 and 1050 mm (Adebayo,

2014), while the minimum temperature in December and January averages 15.2 °C, and the maximum temperature in March and/or April averages about 42 °C (Adebayo and Tukur, 1999). The region has vegetation that is typical of the savannah, including grasslands and sparse trees. The term "cambretaceous woodland savannah" is used to describe the vegetation zone. Grass and weeds make up around 70% of the vegetation, with a few scatted woody species that are native to the area and exotic plants that were introduced from elsewhere. However, human activities such as clearing land for new settlements, farming endeavours, bush burning, and local lumbering have altered the natural vegetation (Adebayo and Tukur, 1999; Peter et. al., 2016).

Data Types and Sources
Level 1 data of Landsat 8 satellite imagery acquired on March 1st, 2021 (path/row: 185/53) was used as input data in this study using the Maths Algebra tool in ArcGIS software. Landsat 8 is one of the Landsat series of NASA which is available on the Earth Explorer website free of cost. It carries two sensors, i.e., the operational land imager (OLI) and the thermal infrared sensor (TIRS). OLI collects data at a 30 m spatial resolution with eight bands located in the visible and near-infrared and the shortwave infrared regions of the electromagnetic spectrum, plus an additional panchromatic band at 15 m spatial resolution. TIRS sensor measures the TIRS radiance at 100 m spatial resolution using two bands located in the atmospheric wavelength window between 10 and 12 μm.

Landsat 8 Satellite Image Data Pre-Processing
To pre-process the satellite images, the digital numbers (DN) of the TIRS and OLI bands were converted to spectral radiance and top of atmosphere (TOA) planetary reflectance. Top-of-atmosphere radiance (L_{ToA}) is first determined using band 10 of the TIRS, and then the at-sensor brightness temperature (BT) estimated. OLI bands 4 (red), and 5 (infrared) are first converted to the reflectivity of the top of the atmosphere and then used to estimate the Normalized Difference Vegetation Index (NDVI). Using the NDVI, the proportion of vegetation (Pv) and the Land Surface Emissivity (LSE) are determined. After that, the radiative transfer equation is used for the estimation of the LST. All these processes were

carried out using the maths algebra Toolbox in ArcGIS software.

Thermal Infrared (TIRS) Image Processing
This image processing can be described as a two-step process. The first step includes the conversion of level-1 DN values of band 10 to at-satellite (or at-sensor, or ToA) spectral radiance values. The formula to convert level-1 DN values to spectral radiance is (USGS):

$$L_{TOA} = M_L \times Q_{cal} + A_L \qquad \text{(i)}$$

where: L_{TOA} is Spectral radiance in watts per metre squared steradian micron (W/(m^2.sr.μm)), M_L is the band-specific multiplicative rescaling factor; Q_{cal} is Band10 pixel value in DN; A_L is the band-specific additive rescaling factor (M_L and A_L can be obtained from the metadata file as 0.0003342 and 0.10000 respectively)

After the digital numbers (DNs) are converted to reflection, the TIRS band data is then converted from spectral radiance to brightness temperature (BT) by assuming the earth's surface as a black body. The conversion formula is (USGS):

$$BT = \frac{K_2}{ln\left(\frac{K_1}{L_\lambda}+1\right)} - 273.15 \qquad \text{(ii)}$$

where: BT is in Kelvin, to obtain the results in Celsius, the radiant temperature is adjusted by adding the absolute zero (approx. -273.15°C), K_1 and K_2 are band-specific thermal conversion constants from the metadata file (K_1 = 774.9853 and K_2 1321.0789). The resulting temperature values are known as black body temperatures, which require spectral emissivity correction based on the type of land cover to be converted to land surface temperatures (Yue et. al., 2007).

Operational Land Imager (OLI) Image Processing
As remote sensing images are subject to cloud cover, atmospheric scattering effects, viewing angle problems, etc., the raw data of the visible red and near-infrared bands (bands 4 and 5 respectively) needs to be converted into surface reflectance values to correct those effects. In practice, the level-1 DN values of bands 4 and 5 are first converted to the reflectivity of the top of the atmosphere by the following equation (USGS):

$$\rho_\lambda = \frac{M_p \times Q_{cal} + A_p}{Sin\theta} \qquad \text{(iii)}$$

Where ρ_λ is the reflectance of the top of the atmosphere at band λ, Mρ and Aρ are the reflectivity adjustment factor of band λ, they can be obtained from the metadata file of Landsat 8, as Reflectance Mult Band and Reflectance Add Band respectively. For bands (4 and 5), the Mρ value is 2.0000×10^{-5} and the Aρ value is -0.100000. θ is solar elevation angle, which is the local sun elevation angle at the time of satellite overpass available in the image metadata file of Landsat 8 as Sun Elevation.

Estimation of Normalized Difference Vegetation Index and the Proportion of Vegetation Cover

The Normalized Difference Vegetation Index (NDVI) is a numerical indicator that uses the visible and near-infrared bands of the electromagnetic spectrum to analyze remote sensing measurements and assess whether the target being observed contains live green vegetation or not (Macarof and Statescu, 2017). Upon the correction of bands 4 and 5, the NDVI is determined using:

$$NDVI = \frac{\rho_{band5} - \rho_{band4}}{\rho_{band5} + \rho_{band4}} \qquad \text{(iv)}$$

Where ρ_{band5} is the reflectance image of the near-infrared band and ρ_{band4} is the reflectance image of the red band.

This proportion of vegetation (Pv) gives the estimation of the area under each land cover type. It is calculated from NDVI as:

$$P_v = \left[\frac{NDVI - NDVI_{min}}{NDVI_{max} - NDVI_{min}}\right]^2 \qquad \text{(v)}$$

Estimation of Land Surface Emissivity (LSE)

The term "Land Surface Emissivity (LSE)" is used to indicate emissivity from land surfaces that are composed of different types of materials (soils, vegetation, water, etc.). It is one of the key parameters needed to retrieve an accurate LST from remotely sensed imagery. It is a proportionality factor that scales blackbody radiance (Planck's law) to predict emitted radiance (Jiménez-Muñoz et al., 2006). Valor and Caselles (1996) proposed a theoretical model that relates the emissivity to the NDVI of a given surface by:

$$\varepsilon = 0.985P_v + 0.960(1 - P_v) + 0.06P_v(1 - P_v) \text{ (vi)}$$

RTE Method for LST Estimation

A methodology for retrieving LST from a single TIRS band is based on the inversion of the following radiative transfer equation (RTE) (Sekertekin and Bonafoni, 2020):

$$L_{ToA} = [\varepsilon B(T_S) + (1 - \varepsilon)L_{down}]\tau + L_{up} \qquad \text{(vii)}$$

where L_{ToA} is the Top of Atmospheric (TOA) radiance of the related thermal band, ε is the land surface emissivity, B(Ts) is the blackbody radiance at a temperature of Ts given by the Planck's law where Ts is the LST, τ is the atmospheric transmissivity between the surface and the sensor, L_{up} and L_{down} are the upwelling and downwelling radiance in the atmosphere respectively,

The blackbody radiance, B(Ts) at a temperature of Ts can be obtained by inverting equation (vii):

$$B(T_S) = \frac{L_{ToA} - L_{up} - \tau(1 - \varepsilon)L_{down}}{\tau\varepsilon} \qquad \text{(viii)}$$

Finally, Ts can be obtained by inverting Planck's law as:

$$LST = \frac{C_2}{\lambda ln\left[\frac{C_1}{\lambda^5\left(\frac{L_{ToA} - L_{up} - \tau(1 - \varepsilon)L_{down}}{\tau\varepsilon}\right)} + 1\right]} \qquad \text{(ix)}$$

The atmospheric parameters (τ, L_{up} and L_{down}) needed to retrieve LST were retrieved from an online atmospheric correction calculator available at https://atmcorr.gsfc.nasa.gov/. This calculator extracts required parameters from NCEP database using MODTRAN codes and the spectral response curve of Landsat 8. The online atmospheric correction tool requires the user to input some mandatory data including location (longitude and latitude), date, and time for which the atmospheric parameters are to calculate. Some optional surface conditions can be input, but if left empty, are assumed from the atmospheric database (Sekertekin and Bonafoni, 2020).

Besides these parameters, land surface emissivity (ε) is necessary.

Results and Discussion

Figure 2 displays the result of this work as a map depicting the spatial distribution of LST across the

study area. As shown in figure 3, the LST of the study area is further classified into two classes (LST values above and below the average value) as presented in figure 3. A comparison was carried out between the LST value calculated at a metrological station situated within the study area and the data of instantaneous near-surface air temperature measured by the metrological instrument on the same day the satellite image used in calculating the LST was obtained.
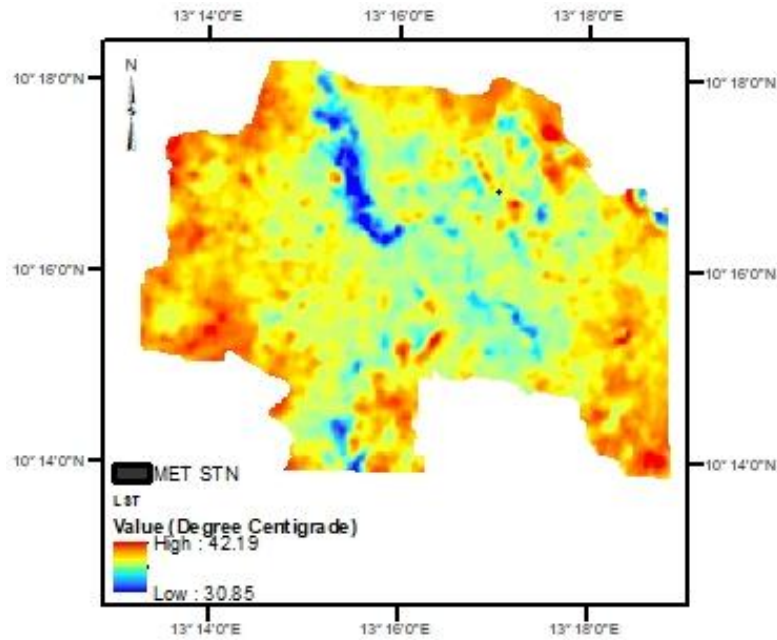

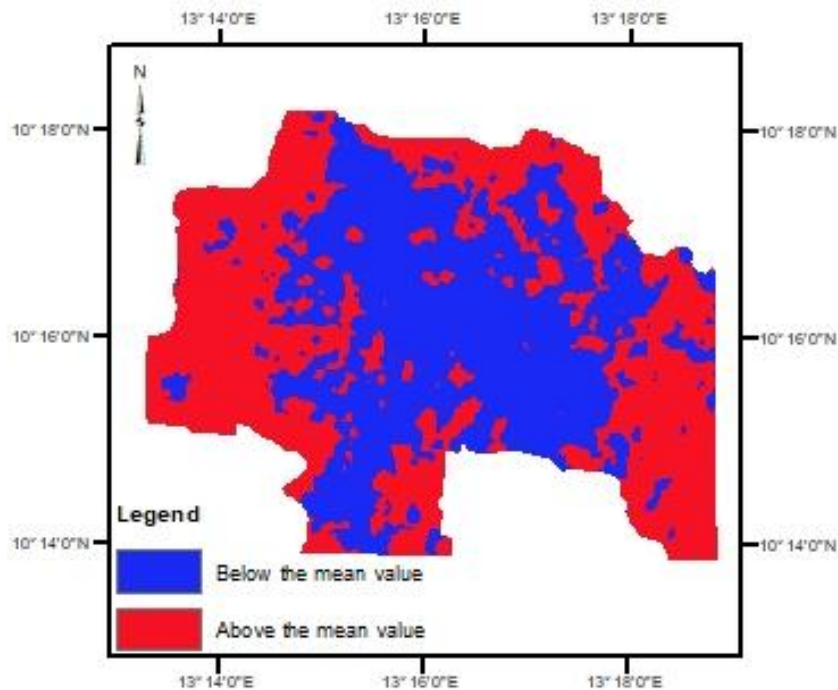**Figure 2:** LST map of the study area

Figure 3: Classify LST map of the study area

The spatial distribution map of LST across Mubi metropolis in figure 2 shows an estimated temperature variation of 30.85 ^{o}C to 42.19 ^{o}C with a mean value of 37.83 ^{o}C. Above-average temperature values are seen in places with a high concentration of bare soil, agricultural fallow land, and little human habitation, typically on the outskirts of the metropolis. Low temperature values below the average are typically found in the city's centre, areas with a lot of buildings and trees, and regions with water bodies and dense vegetation.

Figure 3's classified map reveals that 51% of the study area, which covers an area of approximately 29.55 square km, has a temperature value that is above the average temperature, while 49% of the study area, which covers an area of approximately 28.15 square km, has a temperature value that is below the average.

Since satellite-based thermal infrared sensor data is directly linked to the LST through the radiative transfer equation, the TIRS bands see heat and instead of measuring the temperature of the air, as weather stations do, they report on the ground itself, which is often much hotter (Solanky et al., 2018). Therefore, the result of this work was compared with data of air temperature obtained from the metrological station of Adamawa State University, Mubi, situated in the study area. The LST value for the pixel on which the meteorological station fell was taken and compared with the instantaneous air temperature recorded on the same day and time at which the satellite image used in calculating the LST was obtained. The pixel value of LST at the metrological station is about 37.55 ^{o}C while the metrological instrument recorded an instantaneous near-surface air temperature of 30.80 ^{o}C on that day and time. The difference between the two temperatures is about 6.75 ^{o}C. Depending on the weather condition and other variables such as the resolution of the remote sensing imagery, this difference could be very small or very large. The fact that we are comparing the temperature of the ground surface with that of the air near the Earth's surface, which is often monitored at 1.5 to 2 m off the ground by conventional meteorological stations, may also be a contributing factor (Avdan and Jovanovska, 2016; Gallo et.al., 2011). According to Mutiibwa et. al., (2015), LST cannot be used as a direct substitute for near-surface air temperature, because the two temperatures have different physical meanings, magnitudes, measurement techniques, diurnal phases, and responses to atmospheric conditions. However, there exists a strong relationship between LST and near surface air temperature when daily records are computed over time. The relationship varies with atmospheric, seasonal, and geographical changes. The remotely sensed LST is found to be more valuable in complex mountainous terrain, where it may be used as a proxy or an input variable for estimating the near-surface air temperature because of the paucity of metrological stations in such an environment.

Conclusion

Studying LST has become easier at the local, regional, and global scales with the recent developments in remote sensing earth observation technology. Landsat thermal images can provide researchers with a good, efficient, and time-saving choice for computing land surface temperature. The LST of Mubi metropolis was calculated using the RTE algorithm in the ArcGIS environment. Landsat 8's OLI bands 4 and 5 as well as TIRS band 10 were employed in this study. The research amply reveals a temperature range of 30.85°C to 42.19°C with a mean value of 37.83°C across the studied area. Low temperatures are seen in built-up areas and areas with dense vegetation, whereas high temperatures are estimated in bare soil, agricultural fallow land, and locations with less settlement. The comparative analysis between the LST and the measured near-surface air temperature in the study area during the period under study shows a difference of about 6.75 ^{o}C.

References

Adebayo, A. A (2004). Mubi region: A geographical synthesis (1st ed.), Paraclete Publishers, Yola-Nigeria.

Adebayo, A. A and Tukur, A. L (1999). Adamawa State in Maps (1st ed.), Paraclete publishers Yola-Nigeria.

Anandababu D, Purushothaman B M and Babu S S (2018). Estimation of Land Surface Temperature using LANDSAT 8 Data. International Journal of Advance Research, Ideas and Innovations in Technology. Vol. 4(2), 177-186.

Avdan, U. and Jovanovska, G (2016). Algorithm for Automated Mapping of Land Surface

Temperature Using LANDSAT 8 Satellite Data. J. Sens. Pp 1 -8.

Becker, F.; Li, Z.L. (1990). Toward a local split window method over land surface. Int. J. Remote Sens., 11, 369–393.

Gallo J. K, Hale R, Tarpley D, and Yu Y (2011). Evaluation of the relationship between air and land surface temperature under clear and cloudy sky conditions. Journal of Applied Meteorology and Climatology, vol. 50, no. 3, pp. 767–775.

Jiménez-Muñoz, J.C.and Sobrino, J.A. (2003). A generalized single-channel method for retrieving land surface temperature from remote sensing data. J. Geophys. Res., 109, 8112.

Jiménez-Muñoz, J. C., Sobrino, J. A., Gillespie, A., Sabol, D., and Gustafson, W. T. (2006). Improved land surface emissivities over agricultural areas using ASTER NDVI. Remote Sensing of Environment, 103, 474–487.

Javed, M., Yogesh, K. and Bharath, B.D. (2008) Estimation of Land Surface Temperature of Delhi Using Landsat-7 ETM+. Journal of Industrial Geophysics Union, 12, pp 131-140.

Macarof P and Statescu F (2017). Investigating land surface temperature changes using Landsat data: a case study of Iaşi county. Bul. Inst. Polit. Iaşi, Vol. 63 (67), Nr. 3-4, pp 72 – 79.

Mutiibwa D., Strachan S. and Albright T. P., (2015). Land Surface Temperature and Surface Air Temperature in Complex Terrain. IEEE Journal of Selected Topics in Applied Earth Observations and Remote Sensing, 1-13 https://doi.org/10.1109/JSTARS.2015.24 68594.

Orhan, O., Ekercin, S., and Dadaser-Celik, F. (2014). Use of Landsat Land Surface Temperature and Vegetation Indices for Monitoring Drought in the Salt Lake Basin Area, Turkey. The Scientific World Journal, pp 1–11.

Peter Y, Sheriff E and Garba B. A (2016). Temporal change detection of vegetation cover in Mubi metropolis and environs, Adamawa State, Nigeria. Sky Journal of Soil Science and Environmental Management Vol. 5(3), pp. 059 – 065

Qin, Z.; Karnieli, A.and Berliner, P. (2001). A mono-window algorithm for retrieving land surface temperature from Landsat TM data and its application to the Israel-Egypt border region. Int. J. Remote Sens., 22, 3719–3746.

Rajeshwari, A. and Mani, N.N. (2014) Estimation of Land Surface Temperature of Dindigul District Using Lansat 8 Data, International Journal of Research in Engineering and Technology, 3, 122-126. https://doi.org/10.15623/ijret.2014.03050 25

Sharma V R and Bisht K (2019). Estimation of Land Surface Temperature using LANDS DATA: A case study of Agra city, India. International Journal of Advance Research, Ideas and Innovations in Technology. Vol. 5(2), 1850-1857.

Sekertekin A and Bonafoni S (2020). Land Surface Temperature Retrieval from Landsat 5, 7, and 8 over Rural Areas: Assessment of Different Retrieval Algorithms and Emissivity Models and Toolbox Implementation. Remote Sens., 12, 294.

Sobrino J. A, Jimenez-Munoz J. C, Soria G (2008). Land surface emissivity retrieval from different VNIR and TIRS sensors, IEEE Transactions on Geoscience and Remote Sensing, vol. 46, no. 2, pp. 316–327.

Solanky, V., Singh, S., Katiyar, S.K. (2018). Land Surface Temperature Estimation Using Remote Sensing Data. In: Singh, V., Yadav, S., Yadava, R. (eds) Hydrologic Modeling. Water Science and Technology Library, vol 81. Springer, Singapore. https://doi.org/10.1007/978-981-10-5801-1_24

UKEssays. (November 2018). Applications Of Remote Sensing Environmental Sciences Essay. Retrieved from https://www.ukessays.com/essays/environmental-sciences/applications-of-remote-sensing-environmental-sciences-essay.

U.S. Geological Survey. Landsat 8 (L8) Data Users Handbook, Version 2.0. Available online: https://www.usgs.gov/land-resources/nli/Landsat/Landsat-8-data-users-handbook accessed on 19 March 2022).

Valor, E. and Caselles, V (1996). Mapping land surface emissivity from NDVI:

Application to European, African, and South American areas. Remote Sens. Environ., 57, 167–184.

Yu, X.; Guo, X.;Wu, Z. (2014). Land surface temperature retrieval from Landsat 8 TIRS-comparison between radiative transfer equation-based method, split window algorithm and single channel method. Remote Sens., 6, 9829–9852

Zhou W, Qian Y, Li X, et al. (2014). Relationships between land cover and the surface urban heat island: seasonal variability and effects of spatial and thematic resolution of land cover data on predicting land surface temperatures[J]. Landscape Ecology, 29(1): 153-167.